

First-principles study of temperature-dependent diffusion coefficients for helium in α -Ti

Yong Lu,¹ Fawei Zheng,¹ and Ping Zhang^{1,2,*}

¹*LCP, Institute of Applied Physics and Computational Mathematics, Beijing 100088, People's Republic of China*

²*Beijing Computational Science Research Center, Beijing 100084, People's Republic of China*

The temperature-dependent diffusion coefficients of interstitial helium atom in α -Ti are predicted using the transition state theory. The microscopic parameters in the pre-factor and activation energy of the impurity diffusion coefficients are obtained from first-principles total energy and phonon calculations including the full coupling between the vibrational modes of the diffusing atom and the host lattice. The climbing image nudged elastic band (CINEB) method is used to search for the minimum energy pathways and associated saddle point structures. It is demonstrated that the diffusion coefficients within the xy plane (D_{xy}) is always higher than that along the z axis (D_z), showing remarkable anisotropy. Also, it is found that the formation of helium dimer centered at the octahedral site reduces the total energy and confines the diffusion of helium atoms.

PACS numbers: 63.20.dk, 63.20.D-, 66.30.-h

I. INTRODUCTION

Helium atoms could be produced in metals either through nuclear reactions of energetic particles such as reactor neutrons and light ions or via the radioactive decay of tritium [1]. Due to the closed-shell electron configuration, helium is inactive to metals and has extremely low solubility in metals. Helium atoms diffuse rapidly in the interstitial region until it reaches a trapping site. As the helium concentration increases by direct implantation or neutron transmutation, they tend to agglomerate into helium bubbles when several helium atoms migrate to the same trapping site, which may substantially deteriorate the mechanical properties of metals. Particularly, at high homologous temperatures, helium bubbles can cause intergranular embrittlement, cave, and swelling [2, 3]. Many experimental and analytical investigations of helium bubble growth and helium diffusion in metals have been presented [1–8]. Although the experiments can give the formation energy of helium bubbles and overall diffusion coefficients, generally they cannot determine the microscopic physical processes involved in the formation and diffusion steps, which are quite important for basic understanding and practical applications. First-principles calculations and molecular dynamic simulations, which have been widely used in the study of solid-state diffusion, can help to track the microscopic diffusion processes and give rise to specific quantitative values involved in the atomistic processes, where the experimental measurements cannot reach [9–14].

As an important material to store and retrieve hydrogen, titanium has many important applications in aircraft construction and aerospace engineering, as well as in the chemical industry. While, there are considerable

restrictions in its applications under hydrogen-containing environments. Helium atoms are usually introduced into titanium through tritium decay, then titanium containing tritium becomes doped with ^3He , which tends to agglomerate into bubbles resulting in a severe deterioration in the mechanical properties. At room temperature, titanium exhibits the hexagonal α phase, whereas, it undergoes phase transition from α -phase to β -phase (bcc structure) at the temperature around 1155 K. This relatively low transition temperature for Ti makes diffusion experiments difficult to be solely carried out within the α -phase. Furthermore, due to the insolubility of helium, the knowledge about its diffusion behavior in metals are very few in contrast to other light elements such as H, C, N or O. To date, the experimental diffusion coefficients of helium in α titanium are rather scarce [4], and to our knowledge, systematic *ab initio* studies of hydrogen diffusion in α Ti is still lacking in the literature. The purpose of the present work is to comprehensively investigate the atomic diffusion mechanism of helium in α -Ti, and to obtain the specific values of the corresponding energy barriers and diffusion coefficients from first principles.

II. THEORY AND METHODS

In the most general form, the diffusion coefficient is expressed as

$$D = D_0 e^{-Q/kT}, \quad (1)$$

where Q is the activation energy, D_0 is a pre-factor, and k is the Boltzmann constant. Following the Wert and Zener [15], the diffusion coefficient can be written as

$$D = n\beta d^2\Gamma, \quad (2)$$

where n is the number of nearest-neighbor stable sites for the diffusing interstitial atom, β is the jump probability in the direction of diffusion, d is the length of the jump

*Author to whom correspondence should be addressed. E-mail: zhang-ping@iapcm.ac.cn

projected onto the direction of diffusion, and Γ is the jump rate between adjacent sites of the diffusing atom. According to the transition state theory (TST) [16, 17], the jump rate is written as

$$\Gamma = \frac{kT}{h} \frac{\prod_{i=1}^{3N-6} [1 - \exp(-h\nu_i^0/kT)]}{\prod_{i=1}^{3N-7} [1 - \exp(-h\nu_i^*/kT)]} e^{-\Delta H_m/kT}, \quad (3)$$

where ν_i^* and ν_i^0 are the vibrational frequencies at the transition state and the ground state, respectively. For the high temperature range ($h\nu_i/kT \ll 1$), all vibrational degrees of freedom approach a classical behavior and the jump rate reduces to,

$$\Gamma = \frac{\prod_{i=1}^{3N-6} \nu_i^0}{\prod_{i=1}^{3N-7} \nu_i^*} e^{-\Delta H_m/kT}. \quad (4)$$

For the low temperature range ($h\nu_i/kT \gg 1$), the jump rate can be expressed as [10]

$$\Gamma = \frac{kT}{h} e^{-(\Delta H_m + \Delta E_{zp})/kT}, \quad (5)$$

where E_{zp} is the difference in zero-point energies between ground state and transition state.

Using the phonon free energy at different states

$$F_{vib} = kT \int_0^\infty g(\nu) \ln \left[2 \sinh \left(\frac{h\nu}{2kT} \right) \right], \quad (6)$$

the jump rate can be simply expressed as

$$\Gamma = \frac{kT}{h} e^{-\Delta F_{vib}/kT} e^{-\Delta H_m/kT}, \quad (7)$$

where the zero-point energy is included in the F_{vib} term.

The density functional theory (DFT) calculations are carried out using the Vienna *ab-initio* simulation package (VASP) [18, 19] with the projector-augmented-wave (PAW) potential method [20]. The exchange and correlation effects are described by the local density approximation (LDA). The cutoff energy for the plane-wave basis set is 450 eV. We employ a $3 \times 3 \times 2$ α -Ti supercell containing 36 host atoms to simulate helium migration in the α -Ti matrix. To check the convergence of the formation energies, we have also considered a $4 \times 4 \times 3$ α -Ti supercell containing 96 host atoms and one helium atom. The integration over the Brillouin zone is carried out on $5 \times 5 \times 5$ k -point meshes generated using the Monkhorst-Pack [21] method, which proves to be sufficient for energy convergence of less than 1.0×10^{-4} eV per atom. During the supercell calculations, the shape and size of the supercell are fixed while all the ions are free to relax until the forces on them are less than $0.01 \text{ eV } \text{\AA}^{-1}$. In order to calculate the migration energies of helium in titanium, each saddle-point structure and associated minimum energy pathway (MEP) were calculated by employing the image nudged elastic band (CINEB) method [22]. The vibrational frequencies were computed using the density functional perturbation theory with the help of PHONOPY package [23].

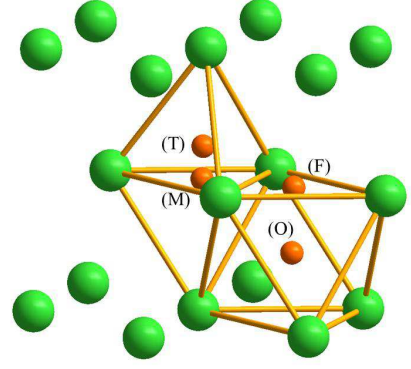


FIG. 1: (Color online) Visual structure of α -Ti matrix marked with tetrahedral (T) site, octahedral (O) site, the center of equilateral trigonal face of octahedron (F) site, and the center of equilateral trigonal face of tetrahedron (M) site. Large green and small red balls represent for titanium atoms and interstitial sites for helium atom, respectively.

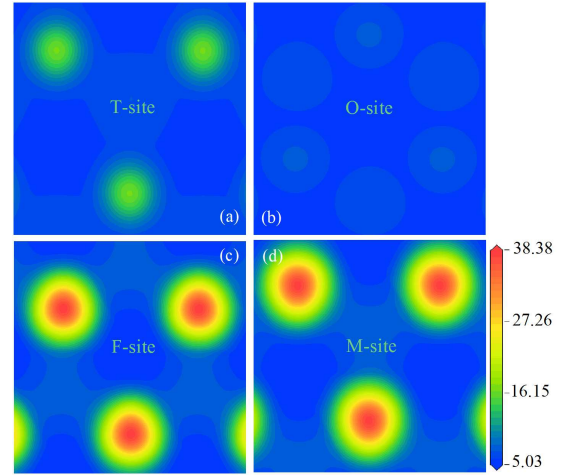


FIG. 2: (Color online) Contour plots of charge density distributions of pure Ti matrix inside the (110) plane crossing T-site (a), O-site (b), F-site (c), and M-site (d), respectively.

III. SOLUTION OF HELIUM ATOM

The formation energy of interstitial helium atom in titanium matrix is calculated by

$$E_f(\text{He}) = E(\text{Ti}, n\text{He}) - n\mu - E(\text{Ti}), \quad (8)$$

where $E(\text{Ti}, n\text{He})$ is the total energy of the supercell containing n interstitial helium atoms, μ is the chemical po-

TABLE I: Calculated formation energy (E_f) for helium atom in various solution sites in hcp-type Ti matrix.

	E_f^T	E_f^O	E_f^F	E_f^M
36-atom cell	2.501	2.746	2.385	2.677
96-atom cell	2.499	2.747	2.382	2.675

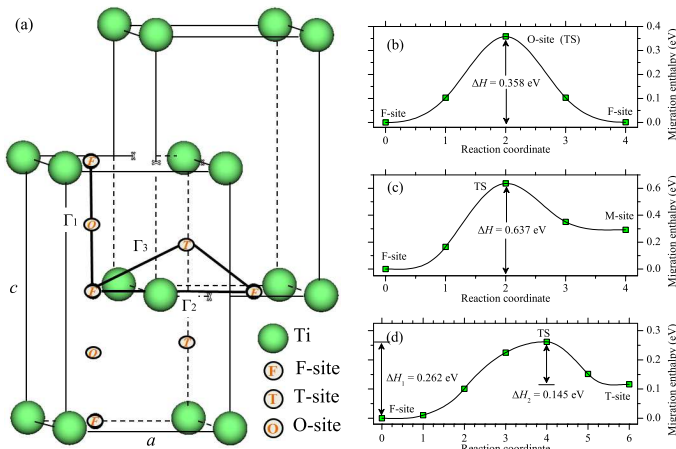


FIG. 3: (Color online) Visual structure of three different jump paths characterized by their jump rates Γ_1 , Γ_2 , and Γ_3 for the He (a), and the reference energy profiles for the He to diffuse along (b) F→O→F, (c) F→M, and (d) F→T paths.

tential of helium atom, $E(\text{Ti})$ is the energy of the Ti supercell without interstitial atoms.

The favorable solution sites for helium atom in metals are those positions of high-symmetry or low charge density. From an intuitional consensus, the octahedral site (O-site) with six nearest Ti atoms and the tetrahedral site (T-site) with four nearest Ti atoms are strong candidates, as marked in Fig. 1. In addition to O-site and T-site, there are two other interstitial sites in the hcp-type Ti matrix, i.e., the center of equilateral trigonal face shared by two adjacent O sites (F-site) and the center of equilateral trigonal face shared by two adjacent T sites along z axis (M-site), as depicted in Fig. 1. We calculated the formation energies of one helium atom in these four types of solution site using the 36-atom model and 96-atom model respectively, and the results are organized in Table I. Clearly, these two models show the similar convergence in energy, implying that the 36-atom supercell is sufficient to assume the simulation task.

The positive formation energies indicate that the dissolution of He in Ti is endothermic. The formation energy of helium in titanium matrix (ranging from 2.385 eV to 2.746 eV) is much lower than that in bcc-type Fe (ranging from 4.22 eV to 5.36 eV) and fcc-type Ni metals (around 4.50 eV) [24–26]. The favorable site in energy for helium atom in titanium matrix is the F-site. Unexpectedly, the O-site, supplying the maximum space for helium atom among the four interstitial sites, has the highest formation energy. This behavior of helium is different from that of H atom in titanium, where O-site is more favorable in energy [27]. To a great extent, the electronic distribution and the interaction between He atom and its surrounding Ti atoms make main contribution in formation energy. Thus, we first plot the charge density of (001) planes crossing the four different sites for pure Ti matrix, as shown in Fig. 2. By comparing the four contour plots of charge density [Figs. 2(a)-(d)], the posi-

TABLE II: Interaction energy (E_{int}) and deformation energy (E_{def}) for helium atom in different solution sites.

	F-site	O-site	T-site	M-site
$E_{int}(\text{He-Ti})$	1.952	2.169	2.074	2.130
$E_{def}(\text{Ti})$	0.432	0.578	0.427	0.547

tion with the lowest charge density is the F-site, and the M-site occupies the highest charge density. The charge density in O-site is somewhat higher than that in F-site, which can be further confirmed by comparing the reference isosurface (not shown here). From the viewpoint of electron distribution, F-site is the most favorable site for helium atom, since the interstitial light elements tend to locate at the site with lowest electron density [28]. Furthermore, we calculated the interaction energy between interstitial helium atom and its surrounding host atoms according to the following expression

$$E_{int}(\text{He} - \text{Ti}) = E(\text{Ti, He}) - E(\text{Ti})^* - E(\text{He}), \quad (9)$$

where $E(\text{Ti, He})$ is the total energy of optimized Ti supercell containing one He atom, $E(\text{Ti})^*$ is the total energy of the supercell containing only Ti atoms with the same atom position and cell parameters as those of $E(\text{Ti, He})$, and $E(\text{He})$ is the energy of one isolate helium atom. The reference results are organized in Table II. Clearly, the interaction energy E_{int} in F-site is the lowest, while the highest energy appears at the O-site. By comparing the energy, the F-site is still the most favorable site for helium atom. The interaction between interstitial helium atom and host atoms will cause the deformation of Ti lattice, further increasing the formation energy. The deformation energy can be evaluated by

$$E_{def}(\text{Ti}) = E(\text{Ti})^* - E(\text{Ti}), \quad (10)$$

and the results are also listed in Table II. Due to the strong interaction between He and Ti atoms, the O-site has the largest deformation energy. The F-site and T-site have low deformation energy, coinciding with the relatively weak interaction between He and host atoms in these two sites.

IV. DIFFUSION IN TITANIUM

From the calculation of formation energy above, we have confirmed that the most favorable site for helium atom in α -Ti matrix is the F-site. In the following, we will investigate the diffusion paths for interstitial helium atom.

As illustrated in Fig. 3 (a), we set the F-site as initial site and choose three candidate jump types characterized by their corresponding jump rates Γ_1 , Γ_2 , and Γ_3 . A diffusive jump of Γ_1 connects two nearest-neighbor F sites in z -axis direction. Γ_2 and Γ_3 are two jump types of helium atom within the basal xy plane, where Γ_2 connects

TABLE III: Calculated electronic energy E_{el} and zero-point energy E_{zp} for interstitial helium atom in 36-Ti matrix. All energies are in kJ/(mol of $\text{Ti}_{36}(\text{He})$). The electronic energy of the elements in their standard states, i.e., Ti_{36} , is taken as reference.

	Ti_{36}	$\text{Ti}_{36}\text{He}(\text{F})$	$\text{Ti}_{36}\text{He}(\text{T})$	$\text{Ti}_{36}\text{He}(\text{O})$	$\text{Ti}_{36}\text{He}(\text{M})$	$\text{Ti}_{36}\text{He}(\text{TS}_{\text{FT}})$	$\text{Ti}_{36}\text{He}(\text{TS}_{\text{FM}})$
E_{el}	0	229.63	240.80	264.49	257.78	254.87	290.99
E_{zp}	119.39	124.98	123.11	113.59	121.82	122.73	121.86

TABLE IV: Calculated diffusion pre-factors (D_0^{xy} and D_0^z) and activation energy (Q_{xy} and Q_z) for helium atom in α -Ti. The temperatures represent the ranges over which diffusion coefficients were fit to extract corresponding pre-factors and activation energies. For comparison, experimental and molecular simulation results are also listed.

Method	D_0^{xy} (m^2/s)	D_0^z (m^2/s)	Q_{xy} (kJ/mol)	Q_z (kJ/mol)	T (K)
This study	5.06×10^{-6}	6.63×10^{-7}	24.48	23.16	280-850
MD ^a	2.1×10^{-8}	2.6×10^{-7}	17.34	17.34	298-667

^a Reference [12]

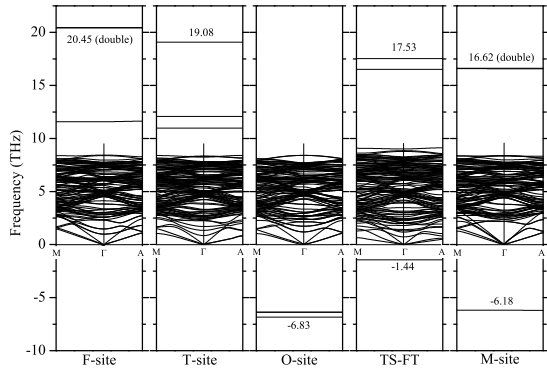


FIG. 4: Calculated phonon dispersions of a 36-atom Ti supercell with helium atom in the F-site, T-site, O-site, M-site and the transition states along the F→T (TS-FT) and F→M (TS-FM) paths, respectively. The modes with imaginary frequencies at the transition states correspond to the motion of the helium atom across the barriers.

these two nearest-neighbor F sites directly and Γ_3 via the T site. We shall determine the more favorable jump type between Γ_2 and Γ_3 by comparing their migration enthalpy. To estimate the migration enthalpy for helium atom diffusion between interstitial sites, the three paths are evenly divided into several segments. We placed He atom at the appropriate position every equal distance. By employing the CINEB method, the activation energy profiles vs diffusion distance are obtained and shown in Figs. 3(b)-(d). For the diffusion path Γ_1 , the energy is found to display a single maximum, corresponding to a saddle point at the high-symmetry position located half way between neighboring F sites, i.e., the O site acts as a transition state role. The energy profile can be well described by a sinusoidal curve with an migration enthalpy of 0.358 eV. For jump Γ_2 , we find that the middle point of diffusion path coincides with M site when the relaxation process completed. Actually, the jump Γ_2 thus connects two nearest-neighbor F sites via the M site. Due to the symmetry of the diffusion curves, we plot here only the

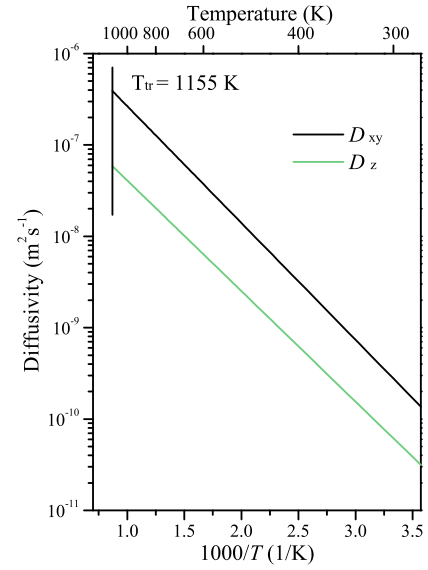


FIG. 5: (Color online) Calculated diffusion coefficients of atomic helium in α -Ti. The $T_{tr}=1155$ K stands for the phase transition temperature of metal Ti from α -phase to β -phase.

ones of F→M for Γ_2 path and F→T for Γ_3 path respectively, as shown in Figs. 3(c) and 3(d). Evidently, the migration enthalpy of the Γ_3 path (0.262 eV) is much lower than that of Γ_2 (0.637 eV). That is, the helium atom tends to diffuse between F sites through the Γ_3 path within the basal xy plane.

The lattice vibrational energy also plays a great role in the migration energy, especially in the high temperature range. In the following, we will calculate the phonon dispersions of these different states using the density functional perturbational theory, and obtain the reference lattice vibrational energy. The $3 \times 3 \times 2$ Ti supercell matrix is employed and one helium impurity is placed at the F-site, T-site, O-site, M-site, and the transition states of F→T (TS-FT), respectively. The phonon dispersions of all these atomic structures including the pure 36-Ti matrix are calculated and shown in Fig. 4. Obviously,

when a helium atom occupies the F site, the He-related phonon dispersions have the highest frequencies, which show a double degenerate dispersionless branch at 20.4 THz. The F site locates at the geometric center of triangle formed by its three nearest Ti atoms, thus the interstitial space is much more confined with respect to other states. At the T site, the highest He-related frequency decreases to 19.1 THz and the degeneracy vanishes. In both cases, the frequencies are positive, indicating a true minimum in the energy. By definition, the transition state is characterized by the occurrence of one negative eigenvalue in the dynamical matrix, showing the imaginary frequency in the phonon dispersion, which corresponds to a motion of helium atom along the diffusion path. When helium locates at the transition state along the F→T path, we note that a Ti-related phonon branch between 8.5 and 9.0 THz is obviously off from the bulk of Ti-related phonon branches. This branch is related to motions of Ti atoms, which couple with motions of the He impurity. At the octahedral site, the He-related branches are all negative, locating at the -6.8 THz nearby. The O-site is the point of maximum solution energy and the helium atom is unstable at this point, tending to diffuse away from it. From the phonon dispersions, we can evaluate the zero-point energy, the temperature dependent enthalpy, and free energy. The electronic energy and zero-point energy of these states are listed in Table III. The zero-point energy at F site is 124.98 kJ/mol, which is the highest one among all the considered states due to the highest He-related branch. With the correction of zero-point energy, the most favorable interstitial site in energy for helium is still the F site at ground state. Finally, we can confirm that the helium atom diffuses in Ti matrix by Γ_1 jump path along the z axis and Γ_3 jump path within the xy plane, respectively.

V. DIFFUSION COEFFICIENTS

Under the assumption of the above jump paths and according to Eq. (2), the two diffusion coefficients in the *hcp*-structured α -Ti can be expressed as

$$D_{xy} = a^2 \Gamma_1 \quad (11)$$

and

$$D_z = \left(\frac{c}{2}\right)^2 \Gamma_3, \quad (12)$$

respectively, where a and c are the lattice parameters of α -Ti. Diffusion coefficient presents more quantitative description on the diffusion features. In Fig. 5 we show the Arrhenius plot, i.e., $\ln(D) = \ln(D_0) - Q/kT$, of the computed diffusion coefficients D_{xy} and D_z . As shown in Fig. 5, the diffusion of helium in α -Ti matrix shows remarkably linear behavior and thus we can obtain the activation energy and prefactor by linear fitting. In Table IV we listed our fitting results of pre-factors and activation energies.

A linear fit between 280 K and 850 K of the calculated data gives $Q_{xy}=24.48$ kJ/mol and $Q_z=23.16$ kJ/mol, both somewhat higher than the molecular dynamic simulation results of 17.34 kJ/mol [12] obtained using the Einstein relation [29]. The diffusion coefficients of these two directions are very anisotropic, corresponding to the pre-factors of $D_0^{xy}=5.06 \times 10^{-6}$ m²/s and $D_0^z=6.63 \times 10^{-7}$ m²/s, respectively. This is consistent with the qualitative observation of helium migration enthalpy, where the helium atom is easier to overcome the migration enthalpy within the xy plane (cf. Fig. 3). Note that the theoretical diffusion coefficients obtained here should be the upper bound of helium migration in α -Ti matrix. Due to the existence of vacancies or dislocations in a real crystal, as well as the formation of helium bubble, the diffusion coefficients will be reduced to some extent. To this end, we also made a relevant test to elaborate the effects of clustering behavior of two helium. We set two helium atoms at the adjacent F sites along the z axis, and then perform the relaxation of the system until the largest force on any atom is smaller than 0.01 eV/Å. We find that two helium atoms form a dimer along the $\langle 001 \rangle$ direction centered at the octahedral site. The formation energy is just 2.05 eV per He atom, lower than that of one helium case (cf. Table I). The formation of helium dimer will confine the diffusion of helium atom in Ti matrix, reducing the diffusion coefficients.

VI. CONCLUSION

In summary, we have systematically studied the temperature-dependent diffusion coefficients of helium atom in α -Ti using transition state theory with accurate first-principles total energy and phonon calculations. It is found that the most stable solution site for He in Ti matrix is the F site, with the lowest formation energy of 2.385 eV. Two minimum energy pathways and associated saddle point structures are determined by using the CINEB method. Within the xy plane, the helium atom diffuses between adjacent solution sites by crossing the T meta-stable site, while along the z axis it should pass the transition state of O site. The obtained diffusion coefficients within the xy plane (D_{xy}) and along the z axis (D_z) show remarkable anisotropy, and the helium atom is more easily to diffuse within the xy plane. The formation of helium dimer centered at the octahedral site reduces the total energy compared to the case of two isolate helium atoms, which confines the diffusion of helium and further reduce the diffusion coefficients. Without considering the vacancies or helium bubble effects, our theoretical diffusion coefficients should be an upper bound on the helium diffusion in Ti matrix, which provides a good reference for future experimental measurements on α -Ti.

Acknowledgments

Science and Technology under Grant No. 2011A0301016.

This work was supported by NSFC under Grant No. 51071032 and by CAEP Foundations for Development of

-
- [1] V. Sciani, P. Jung, Radiation Effects **78** 87-99 (1983).
 - [2] H. Schroeder and P. Batfalsky, J. Nucl. Mater. **103-104**, 839 (1981).
 - [3] H. Trinkaus, B.N. Singh, J. Nucl. Mater. **323** 229 (2003).
 - [4] R. Vassen, H. Trinkaus and P. Jung, J. Nucl. Mater. **183** 1 (1991).
 - [5] G.J. Thomas, W.A. Swansiger and M.I. Baskes, J. Appl. Phys. **50** 6942 (1979).
 - [6] B.N. Singh, H. Trinkaus, J. Nucl. Mater. **186**, 153-165 (1992).
 - [7] R. Rajaraman, B. Viswanathan, M.C. Valsakumar, and K.P. Gopinathan, Phys. Rev. B **50**, 597-600 (1994).
 - [8] B. Glam, S. Eliezer, D. Moreno, D. Eliezer, J. Nucl. Mater. **392** 413-419 (2009).
 - [9] W.D. Wilson, C.L. Bisson and M.I. Baskes, Phys. Rev. B **24** 5616 (1981).
 - [10] E. Wimmer, W. Wolf, J. Sticht, and P. Saxe, Phys. Rev. B **77** 134305 (2008).
 - [11] M. Mantina, Y. Wang, R. Arroyave, L. Q. Chen, Z. K. Liu, and C. Wolverton, Phys. Rev. Lett. **100** 215901 (2008).
 - [12] M. Chen, Q. Hou, J. Wang, T.Y. Sun, X.G. Long, S.Z. Luo, Solid State Commun. **148** 178-181 (2008).
 - [13] M. Mantina, Y. Wang, L. Q. Chen, Z. K. Liu, and C. Wolverton, Acta Mater. **57** 4102-4108 (2009).
 - [14] B.L. Zhang, J. Wang, and Q. Hou, Chin. Phys. B **20** 036105 (2011).
 - [15] C. Wert and C. Zener, Phys. Rev. **76**, 1169 (1949).
 - [16] H. Eyring, J. Chem. Phys. **3**, 107 (1935).
 - [17] G. H. Vineyard, J. Phys. Chem. Solids **3**, 121 (1957).
 - [18] G. Kresse and D. Joubert, Phys. Rev. B **59**, 1758 (1999).
 - [19] G. Kresse and J. Furthmüller, Phys. Rev. B **54**, 11169 (1996).
 - [20] P. E. Blöchl, Phys. Rev. B **50**, 17953 (1994).
 - [21] H. J. Monkhorst and J. D. Pack, Phys. Rev. B **13**, 5188 (1976).
 - [22] G. Henkelman, B. P. Uberuaga, and H. Jonsson, J. Chem. Phys. **113**, 9901 (2000).
 - [23] A. Togo, F. Oba, and I. Tanaka, Phys. Rev. B **78**, 134106 (2008).
 - [24] W.D. Wilson, R.A. Johnson, in: P.C. Gehlen, J.R. Beeler, R.I. Jaffee (Eds.), Interatomic Potentials und Simulation of Lattice Defects, Plenum Press, New York, p. 375, (1972).
 - [25] C.C. Fu, F. Willaime, Phys. Rev. B **72** 064117 (2005).
 - [26] T. Seletskiaia, Y. Osetsky, R. E. Stoller, and G. M. Stocks, Phys. Rev. Lett. **94**, 046403 (2005).
 - [27] Y. Lu, P. Zhang, J. Appl. Phys. **113**, 193502 (2013).
 - [28] J.K. Nørskov, Phys. Rev. B **26** 2875-2885 (1982).
 - [29] G. Boisvert, L.J. Lewis, Phys. Rev. B **54** 2880 (1996).